

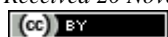
Deciphering Metabolite–MRGPRD interactions: A computational insight into RAS pathway modulation

Neelam Krishna, Shraddha Vishwakarma, Pramod Katara

Centre of Bioinformatics, IIDS, University of Allahabad, Prayagraj-21002, UP, India

E-mail: pmkatara@gmail.com, pkatara@allduniv.ac.in

Received 20 November 2025; Accepted 30 December 2025; Published online 3 January 2026; Published 1 September 2026



Abstract

The renin–angiotensin system (RAS) regulates diverse physiological processes, making it a highly complex and tightly controlled biological network. RAS components signal through two major pathways that mediate both proliferative and anti-proliferative effects. Dysregulation of this system has been implicated in cardiovascular and renal disorders, as well as in SARS-CoV-2 infection. Mas-related G protein-coupled receptor member D (MRGPRD), an emerging RAS-associated protein, has been linked to multiple physiological conditions, including cancer progression and blood pressure regulation. Lacto-tripeptides—bioactive peptides derived from milk—are known modulators of ACE activity and can influence RAS-mediated blood pressure control. In this study, structure-based virtual screening was performed using 206 cow-milk metabolites docked against the MRGPRD receptor. The top-ranked metabolite–protein complex was further examined using molecular dynamics simulations (150 ns) to assess interaction stability and structural dynamics. Among the screened metabolites, BMDB0012305 demonstrated the highest binding affinity and is reported to possess inhibitory potential toward MRGPRD. Molecular dynamics analyses (RMSD, RMSF, and Rg) revealed that the “MRGPRD–BMDB0012305” complex remained stable throughout the simulation, supported by persistent intermolecular interactions such as hydrogen bonding. Overall, our findings suggest that the milk-derived metabolite BMDB0012305 may interact with and modulate MRGPRD function, potentially influencing downstream RAS-related physiological processes. This highlights the need for further experimental validation to understand its biological impact and potential role in RAS-associated abnormalities

Keywords renin angiotensin; MRGPRD; molecular docking; milk metabolites; MD simulation.

Network Biology
ISSN 2220-8879
URL: <http://www.iaees.org/publications/journals/nb/online-version.asp>
RSS: <http://www.iaees.org/publications/journals/nb/rss.xml>
E-mail: networkbiology@iaees.org
Editor-in-Chief: WenJun Zhang
Publisher: International Academy of Ecology and Environmental Sciences

1 Introduction

The renin–angiotensin system (RAS) is a complex regulatory network essential for maintaining cardiovascular, pulmonary, and immune homeostasis in humans (Gomez et al., 2018). Extensive research has characterized two major RAS signaling axes that mediate the proliferative effects of angiotensin II and the

counter-regulatory, anti-proliferative actions of other RAS hormones (Kanugula et al., 2023). Disruption of the balance between these axes contributes to the pathogenesis of several disorders, including cardiovascular diseases and COVID-19 caused by SARS-CoV-2 (Sriram et al., 2020). Aberrant expression of RAS components has also been reported in multiple cancers, including breast cancer, highlighting the system's relevance to tumor biology and the need for novel therapeutic approaches (Galiè, 2019).

The RAS network consists of several G protein-coupled receptors (GPCRs)—AT1R, AT2R, MASR, and MRGPRD—that orchestrate the physiological effects of angiotensin II and angiotensin-(1–7). These hormones are generated by ACE1 and ACE2 through protease-mediated processing (Forrester et al., 2018; Krishna et al., 2024a). Among these receptors, Mas-related G protein-coupled receptor member D (MRGPRD) is part of the larger MAS-related GPCR family, which regulates diverse signaling processes and is implicated in numerous pathological conditions (Etelvino et al., 2014; Bader et al., 2014; Krishna et al., 2024b). Its protein-protein interaction (PPI) network MRGPRD displays his central role in different biological process. Variants and dysregulated signaling of MRGPRD have been associated with disorders such as femoral cancer, Fox–Fordyce disease, and other disease states (Steele & Han, 2021). Increasing evidence suggests beneficial roles for this receptor in cardiovascular and metabolic health, underscoring its potential as a therapeutic target.

Given the central involvement of RAS in systemic vascular resistance, fluid and electrolyte balance, and blood pressure regulation (Fountain et al., 2024), various natural products—including herbs, milk components, and Ayurvedic preparations—have long been explored for their antihypertensive properties. Bioactive milk peptides, including lacto-tripeptides, are known to influence angiotensin-converting enzyme (ACE) activity; however, evidence from human studies remains inconsistent, and their mechanisms of action may extend beyond ACE inhibition (Rubak et al., 2020; Ferrari & Fox, 2009; Fekete et al., 2015). Increasing dietary intake of dairy products has been associated with reduced blood pressure and improved cardiovascular outcomes, potentially through interactions with RAS components (Park & Cifelli, 2013; Timon et al., 2020). Moreover, RAS involvement in inflammation and tissue damage raises the possibility that dietary metabolites could also modulate inflammatory processes via this pathway (Benigni et al., 2010; Cantero-Navarro et al., 2021).

Despite increasing evidence of bioactive components in dairy products, the precise molecular interactions between cow-milk metabolites and human renin-angiotensin system (RAS) proteins remain insufficiently characterized. Bridging this knowledge gap is crucial for understanding potential dietary influences on RAS-mediated physiological processes and disease mechanisms. Bioinformatics tools offer robust structure-based approaches—such as virtual screening and molecular dynamics (MD) simulations—to elucidate binding affinity, stability, and conformational behaviour of biomolecular complexes (Katara, 2014; Zhang, 2018; Pandey et al., 2020; Kumar et al., 2022; Dixit et al., 2024).

In this study, we employed an integrative structure-based workflow to characterize the interaction landscape between cow-milk metabolites and MRGPRD, an important receptor associated with the extended RAS pathway. Virtual screening was first applied to evaluate metabolite binding affinities, followed by the construction of molecular interaction networks to identify key interaction nodes and patterns. MD simulations were then performed to assess the structural stability and dynamic behavior of the top-ranked complex, BMDB0012305–MRGPRD.

Our results demonstrate that the milk-derived metabolite BMDB0012305 exhibits strong and specific binding affinity toward MRGPRD, modulating its conformational dynamics and indicating potential inhibitory activity. These findings provide novel insights into the molecular basis of milk metabolite interactions with RAS-associated receptors and establish a framework for future studies aimed at exploring therapeutic opportunities related to MRGPRD dysfunction.

2 Materials and Methodology

2.1 Selection of Cow-Milk Metabolites

A total of 206 cow-milk metabolites were retrieved from the Bovine Metabolome Database (BMDB, Foroutan et al., 2020) available at, <https://bovinedb.ca/>. These metabolites exhibit diverse physicochemical properties. For structure-based interaction profiling, the 3D structures of all metabolites were downloaded and stored in pdb format for subsequent molecular docking analyses.

2.2 Retrieval of Protein Structure

The 3D structure of the human MRGPRD (UniProt accession: Q8TDS7) receptor was obtained from the Protein Data Bank (PDB; <https://www.rcsb.org/>). The highest-quality available crystal structure (PDB ID: 7Y12, Suzuki, et al., 2022) was downloaded in pdb format and used as the receptor model for docking studies.

2.3 Protein and Ligand Preparation

Both the receptor and ligand structures were prepared for docking-based virtual screening. Initial structural inspection of the receptor, including evaluation of chains, ligands, and ions, was conducted using UCSF Chimera. Protein preparation was then performed using AutoDock Tools (ADT) following standard protocols: (1) Removal of crystallographic water molecules, (2) Addition of all hydrogen atoms, (3). Correction of missing atoms or irregular ions, (4). Assignment of Gasteiger partial charges, and (5). Conversion of the prepared protein structure to pdbqt format

Similarly, ligand structures (milk metabolites) were processed using Open Babel, where atom types and charges were assigned, and the final files were converted to the pdbqt format, required for AutoDock-based docking.

2.4 Molecular Docking

Structure-based docking was performed using AutoDock Vina (Trott & Olson et al., 2010), with the entire surface of the MRGPRD protein considered as the search space. All 206 cow-milk metabolites were docked individually against the MRGPRD receptor. Binding affinities and interaction conformations were recorded for downstream selection and analysis.

2.5 Molecular Dynamics (MD) Simulation

To evaluate the dynamic stability and interaction behavior of the top-scoring complex, atomistic MD simulations were performed for the MRGPRD–BMDB0012305 complex using GROMACS 2020.3 and the CHARMM36 force field (Guterres et al, 2021). Ligand topology files were generated using the CGenFF server.

The prepared complex was: Positioned at the center of a dodecahedral simulation box with a 2 nm margin, Solvated using the SPCE water model, and Neutralized by replacing water molecules with appropriate Na⁺ counterions.

Energy minimization was conducted using the steepest descent algorithm until reaching a tolerance of 1000 kJ/mol/nm. The system was equilibrated, followed by a 150 ns production MD run. Random initial velocities for the first and second replicas were set to -1 and -2 , respectively.

2.6 Trajectory Analysis

MD simulation trajectories were analyzed using Xmgrace for data visualization (Turner, 2005). Four major dynamic parameters, (i.e., RMSD, RMSF, Rg and hydrogen bonding profile), were calculated to assess the stability and flexibility of the complex. These analyses provided insights into the structural stability and interaction dynamics of the MRGPRD–BMDB0012305 complex (Fig. 1).

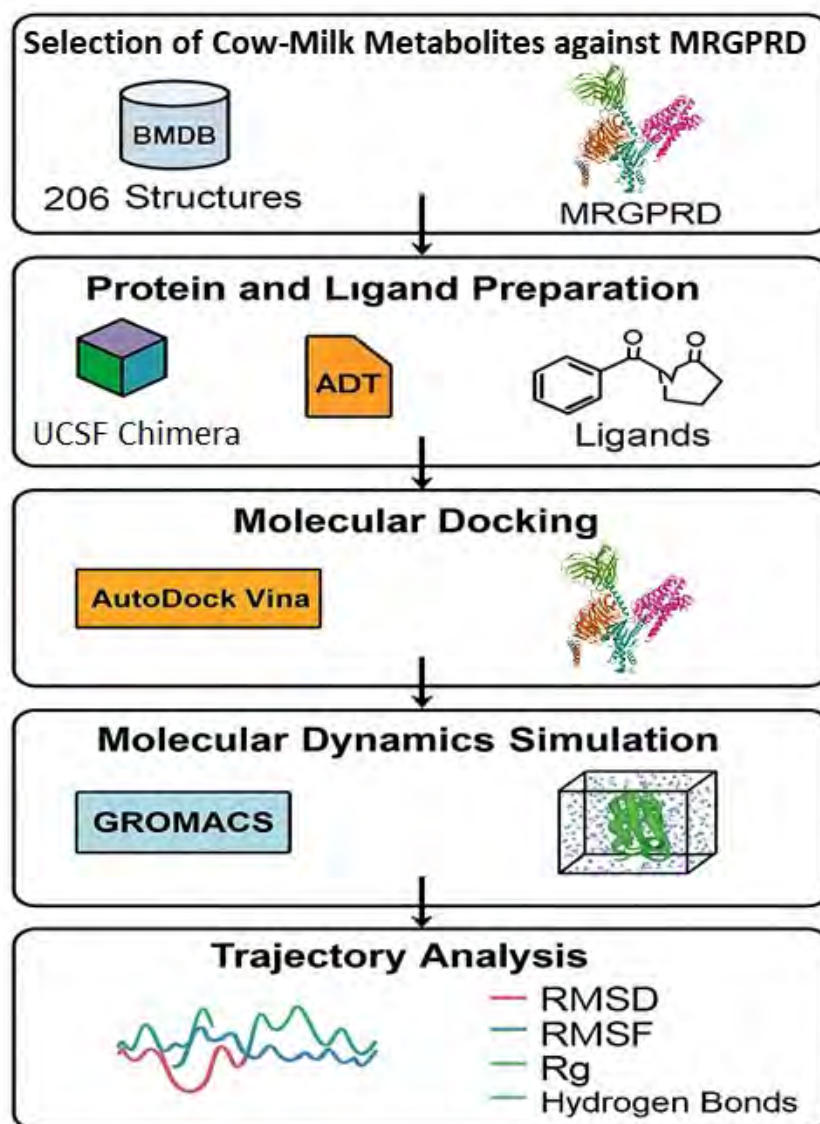


Fig. 1 Schematic representation of considered methodology.

3 Results and Discussion

Milk contains a diverse array of metabolites that contribute to its biological functions and health-related activities. Understanding how these metabolites interact with key human proteins is essential for assessing their potential physiological impacts. In this study, we examined the interaction between the RAS-pathway receptor MRGPRD and cow-milk metabolites to determine whether such interactions may influence receptor behavior and potentially contribute to abnormal physiological outcomes. Further investigation into these protein–ligand interactions is crucial for elucidating their functional relevance and mechanistic roles. To explore these interactions, blind molecular docking was performed using AutoDock Vina, in which MRGPRD was screened against all 206 selected milk metabolites.

3.1 Molecular Docking Analysis

MRGPRD, a receptor associated with the renin–angiotensin system, was selected as the target protein, and its binding affinity toward milk metabolites was evaluated. Docking scores, expressed as binding free energies (kcal/mol) along with RMSD values, were used to assess the strength and stability of metabolite–protein

interactions. Among the 206 metabolites screened, 15 exhibited binding affinities stronger than -8 kcal/mol, indicating a notable interaction with MRGPRD.

Several metabolites demonstrated particularly strong binding propensities, including BMDB0012305, BMDB0002174, BMDB0063639, BMDB0005781, BMDB0001095, and BMDB0063640, each possessing distinct physicochemical characteristics (Table 1). Of these, BMDB0012305 displayed the highest binding affinity (-11 kcal/mol), suggesting it may have a significant inhibitory or modulatory effect on MRGPRD.

Docking analyses revealed that most metabolite-binding regions are located on accessible surface pockets of MRGPRD, consistent with typical ligand–receptor interaction patterns. These interactions are influenced by the physicochemical properties of both metabolites and the receptor, including polarity, molecular size, and hydrogen-bonding capacity. Notably, many of the interacting milk metabolites exhibit favorable ADME-related characteristics—such as suitable solubility, stability, and molecular flexibility—which may further support their potential biological relevance.

Table 1 Summary of milk metabolites exhibiting strong binding to MRGPRD (binding score < -8 kcal/mol) and their physicochemical properties.

SN.	MCDB ID of metabolite	Drugbank ID	Binding affinity	Molecular Weight (g/mol)	HBD count	HBA counts	Rotatable bond
1	BMDB0012305	N/A	-11	550.3	8	16	8
2	BMDB0001341	N/A	-10.7	427.20	4	14	6
3	BMDB0063640	DB00759	-10.1	444.43	6	9	2
4	BMDB0001341	N/A	-9.9	427.20	4	14	6
5	BMDB0002338	N/A	-8.7	284.26	2	3	2
6	BMDB0003429	N/A	-8.7	1329.3	9	19	16
7	BMDB0000429	N/A	-8.5	272.4	2	2	0
8	BMDB0005808	N/A	-8.5	268.26	1	4	2
9	BMDB0000900	DB00153	-8.5	396.6	1	1	5
10	BMDB0000175	DB04566	-8.4	348.21	5	10	4
11	BMDB0001081	N/A	-8.2	463.4	7	10	5
12	BMDB0063637	DB01060	-8.3	365.4	4	7	4
13	BMDB0000067	DB04540	-8.3	386.7	1	1	5
14	BMDB0000077	DB01708	-8.1	288.4	1	2	0
15	BMDB0063639	N/A	-8.1	916.1	5	18	13

3.2 MRGPRD (Mas-Related G-Protein Coupled Receptor Member D)

Docking analysis of MRGPRD revealed that 15 milk metabolites exhibited strong binding affinity toward the receptor, each with binding energies lower than -8 kcal/mol. Among these, BMDB0012305 demonstrated the highest affinity (-11 kcal/mol) (Fig. 2). CavityPlus analysis confirmed that BMDB0012305 occupies the primary binding cavity of MRGPRD, engaging 13 key residues and forming five stable hydrogen bonds. These interactions were complemented by three electrostatic interactions and several carbon–hydrogen contacts (Table 2), indicating a robust and multifaceted binding environment. The electrostatic interactions included

cation- π and π -anion contributions, which further stabilized the ligand-receptor complex. Notably, hydrogen bonds involving VAL276-HN1 and HIS213-HE3 were among the most significant contributors to binding stability.

MRGPRD encodes a G protein-coupled receptor predominantly expressed in sensory neurons, where it plays essential roles in detecting inflammatory signals, transmitting nociceptive information, and mediating itch responses (Jiang et al., 2022). The metabolite BMDB0012305, a nucleotide-sugar molecule, is a key precursor in the biosynthesis of rhamnose, a monosaccharide widely found in biological systems. Rhamnose and its derivatives contribute to the formation of glycoproteins, cell-wall components, and secondary metabolites, making BMDB0012305 central to various metabolic processes required for healthy cellular function. Its incorporation into biological structures occurs through the action of rhamnose transferases, enzymes responsible for transferring rhamnose residues to target molecules (Li et al., 2022).

Previous studies have shown that MRGPRD is a major mediator of LPS-induced chronic inflammation and hyperalgesia, linking this receptor to long-lasting pain and inflammatory responses within the RAS pathway (Li et al., 2020). The strong interaction observed between BMDB0012305 and MRGPRD in this study raises the possibility that certain milk-derived metabolites may influence MRGPRD-associated signaling, potentially modulating inflammatory or sensory outcomes.

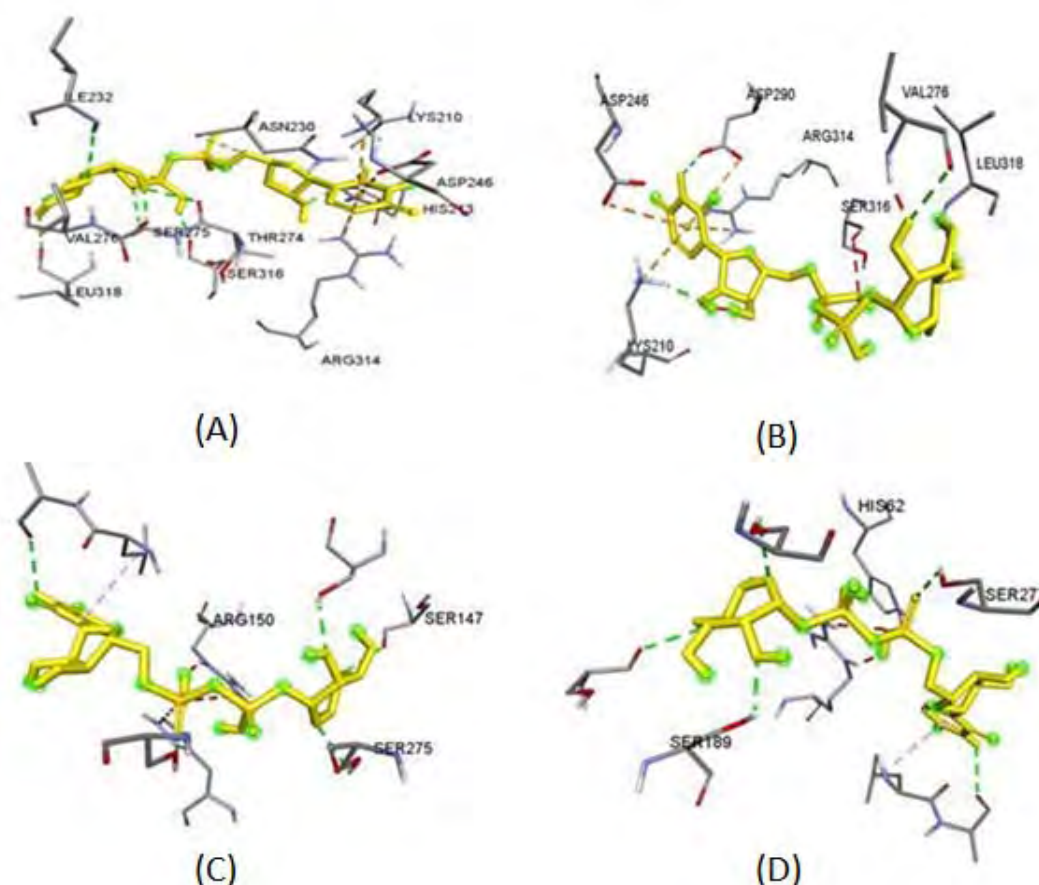


Fig. 2 Best docked sites of MRGPRD against milk metabolite, BMDB0012305. Interaction types: green dashed (H-bond), purple dashed (hydrophobic), orange dashed (electrostatic), red dashed (unfavorable). Panels: A–D show the top four poses in descending order.

Table 2 Details of interacting residues, bond types, and distances for the top four docked (MRGPRD -BMDB0012305) poses, presented in descending order and corresponding to Fig. 2.

Pose	Interacted residues	Bonds	Distance
A	A:HIS213:HE2 - :UNL1:O	Hydrogen Bond	1.9767
	A:HIS213:HE2 - :UNL1:O	Hydrogen Bond	2.93095
	B:ILE232:HN - :UNL1:O	Hydrogen Bond	2.95209
	B:SER275:HG - :UNL1:O	Hydrogen Bond	2.63237
	:UNL1:H - B:SER316:O	Hydrogen Bond	2.11404
	:UNL1:H - B:THR274:O	Hydrogen Bond	3.01686
	:UNL1:H - B:SER275:OG	Hydrogen Bond	2.05813
	:UNL1:H - B:VAL276:O	Hydrogen Bond	1.92037
	:UNL1:H - B:LEU318:O	Hydrogen Bond	2.37855
	:UNL1:C - B:ASN230:O	Hydrogen Bond	3.73258
	A:LYS210:NZ - :UNL1	Electrostatic Bond	3.92959
	B:ARG314:NH1 - :UNL1	Electrostatic Bond	3.59408
	B:ASP246:OD1 - :UNL1	Electrostatic Bond	4.01541
B	A:LYS210:HZ2 - :UNL1:O	Hydrogen Bond	2.03651
	:UNL1:H - B:VAL276:O	Hydrogen Bond	2.65797
	:UNL1:H - B:ASP290:OD2	Hydrogen Bond	2.77989
	A:LYS210:NZ - :UNL1	Electrostatic Bond	4.12934
	B:ARG314:NH1 - :UNL1	Electrostatic Bond	3.56054
	B:ASP246:OD2 - :UNL1	Electrostatic Bond	4.48728
C	B:ASP290:OD1 - :UNL1	Electrostatic Bond	4.71722
	B:ARG150:HH21 - :UNL1:O	Hydrogen Bond	2.23942
	B:SER191:HG - :UNL1:O	Hydrogen Bond	2.75589
	B:PHE234:HN - :UNL1:O	Hydrogen Bond	2.31712
	B:ARG314:HH11 - :UNL1:O	Hydrogen Bond	2.58361
	:UNL1:H - :UNL1:O	Hydrogen Bond	2.74155
	:UNL1:H - B:LEU318:O	Hydrogen Bond	2.03111
	:UNL1:H - B:MET188:O	Hydrogen Bond	2.54384
D	:UNL1:H - B:MET188:O	Hydrogen Bond	1.93927
	:UNL1:C - B:SER275:OG	Hydrogen Bond	3.62796
	B:SER189:HG - :UNL1:O	Hydrogen Bond	2.17803
	B:SER275:HG - :UNL1:O	Hydrogen Bond	2.98022
	B:SER277:HG - :UNL1:O	Hydrogen Bond	2.45169
	:UNL1:H - B:SER147:O	Hydrogen Bond	2.79431
	:UNL1:H - B:ALA193:O	Hydrogen Bond	2.79243
	:UNL1 - B:LEU192	Hydrophobic Bond	4.64712

3.3 MD Simulation of the Docked Complex ‘BMDB0012305–MRGPRD’

Molecular dynamics (MD) simulations were performed to assess the conformational stability and interaction behaviour of the BMDB0012305–MRGPRD complex under dynamic, physiologically relevant conditions. Four key parameters—root mean square deviation (RMSD), root mean square fluctuation (RMSF), radius of gyration

(R_g), and hydrogen-bonding patterns—were analyzed to characterize the stability, flexibility, and compactness of the complex.

The interaction profile revealed that complex stability is governed by a synergistic combination of hydrogen bonding, hydrophobic interactions, and electrostatic forces (Fargher et al., 2022; Sun, 2022). Hydrogen bonds provided directional stability within the binding pocket, hydrophobic contacts shielded nonpolar surfaces from solvent exposure, and electrostatic interactions supported ligand accommodation by facilitating charge complementarity. Together, these forces contributed to a tightly bound and stable complex. Comparative analysis also indicated that the BMDB0012305–MRGPRD complex exhibited greater structural stability than the APO (ligand-free) receptor across the simulation period, suggesting that ligand binding stabilizes MRGPRD.

3.3.1 Root Mean Square Deviation (RMSD)

RMSD analysis is a fundamental metric for evaluating conformational convergence and structural stability in MD simulations (Maruyama et al., 2023). The RMSD profile of the BMDB0012305–MRGPRD complex (Fig. 3) showed initial fluctuations during the early stages of simulation, reflecting structural adjustment as the ligand settled into the binding cavity. Subsequently, the RMSD values stabilized, ranging between 0.1 nm and 0.3 nm, indicating sustained structural integrity throughout the 150 ns simulation.

In contrast, the APO form displayed larger deviations, signifying higher intrinsic flexibility and reduced stability in the absence of a ligand. The higher RMSD observed for the native structure indicates that BMDB0012305 binding promotes a more stable, energetically favorable conformation. The RMSD plateau also suggests that the complex achieves equilibrium after initial rearrangements.

Overall, RMSD analysis highlights subtle yet meaningful conformational changes induced by ligand binding and confirms the formation of a stable, well-defined protein–ligand complex.

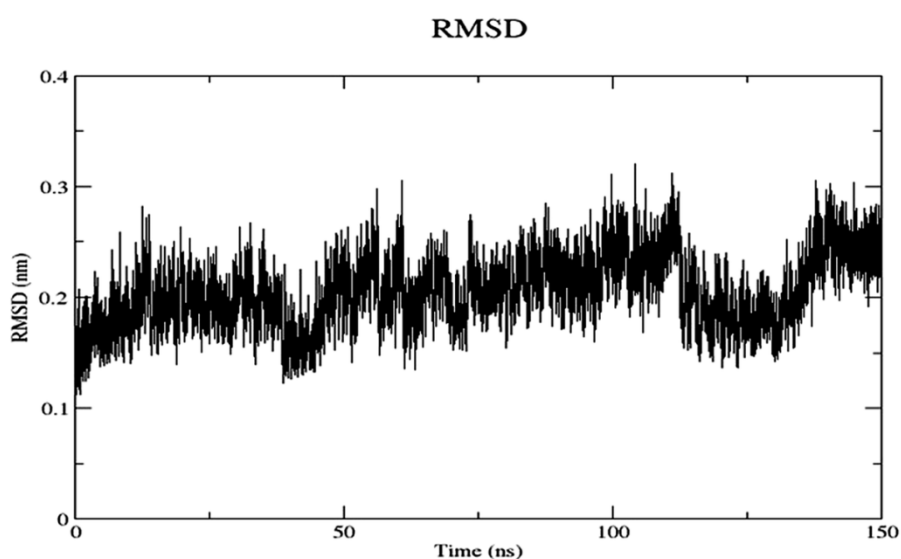


Fig. 3 RMSD profile of the BMDB0012305–MRGPRD complex over the simulation period.

This observation suggests that the protein's structure attained a specific distance from the reference structure and subsequently maintained a relatively constant distance in comparison to the reference structure.

3.3.2 Root Mean Square Fluctuations

The Root Mean Square Fluctuation (RMSF) analysis quantifies the extent of atomic displacement around each residue's mean position, providing insight into local flexibility and thermodynamic stability. Higher RMSF values

indicate regions of increased mobility, whereas lower values reflect more rigid and structurally stable regions (Ghahremanian et al., 2022).

In this study, the RMSF profile revealed distinct patterns of intrinsic flexibility within the MRGPRD structure. These fluctuations closely correlated with the crystallographic B-factors (temperature factors), which represent average atomic displacement within the crystal lattice. The strong correspondence between RMSF and B-factor values supports the reliability of the simulation and enhances our understanding of residue-level dynamics. This alignment confirms that the simulated structural motions accurately reflect the protein's inherent flexibility and stability at the atomic scale.

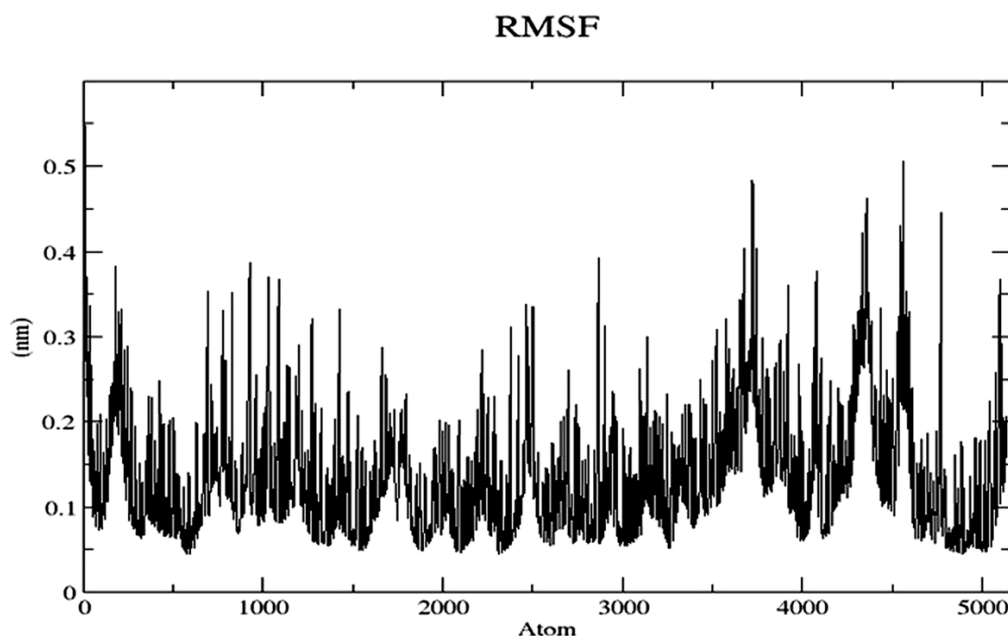


Fig. 4 Root mean square fluctuation (RMSF) analysis of the BMD0012305–MRGPRD complex showing residue-level flexibility during the simulation.

To assess the agreement between the simulation results and the experimentally derived crystal structure, a correspondence analysis was performed. The RMSF profile clearly demonstrates that the highest fluctuations occur at the N- and C-terminal regions, which is expected, as terminal segments typically exhibit greater intrinsic flexibility in GPCRs and many other proteins. The backbone residues of the BMD0012305–MRGPRD complex showed fluctuations within the range of 0.1 nm to 0.0 nm (Fig. 4), indicating moderate and biologically consistent mobility across the protein structure

3.3.3 Radius of Gyration (Rg)

The radius of gyration (Rg) provides important insights into the overall compactness and conformational stability of a protein during molecular dynamics simulations. Rg reflects the distribution of atomic mass around the protein's center of mass and is closely related to the experimentally measurable hydrodynamic radius. Lower Rg values generally indicate a more compact, folded, and stable structure, whereas higher values suggest expanded or partially unfolded conformations (Sneha & Doss, 2016).

Ligand binding often induces conformational adjustments in proteins that may influence structural integrity and functional behavior (Di, 2020). In the present study, the Rg profile of the BMD0012305–MRGPRD complex remained within a narrow range of 2.05 to 2.20 nm throughout the simulation (Fig. 5), reflecting a stable and compact structure. A slight initial increase in Rg was observed as the receptor accommodated the ligand, after which the complex rapidly stabilized.

In contrast, the APO (ligand-free) form exhibited greater fluctuations, indicating reduced structural stability compared to the ligand-bound complex. These observations suggest that binding of BMDB0012305 enhances the conformational stability of MRGPRD and supports the overall structural integrity of the receptor during the simulation.

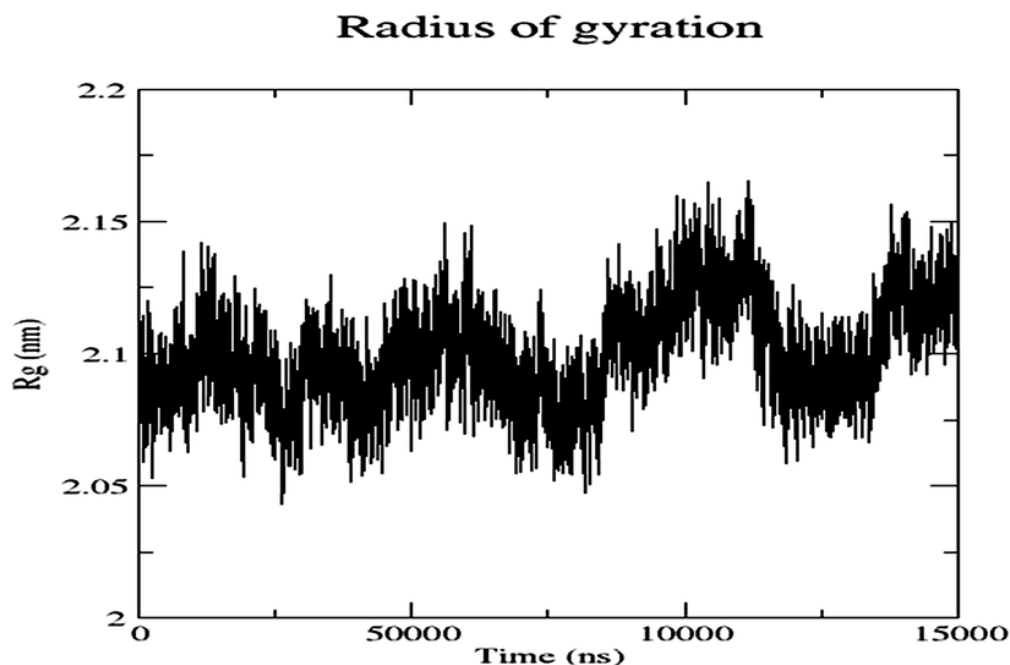


Fig. 5 Radius of gyration (R_g) profile illustrating the structural compactness of the BMDB0012305–MRGPRD complex during the simulation.

3.3.4 Hydrogen Bond Interaction

Intermolecular hydrogen bonds are key determinants of specificity and affinity in protein–ligand interactions. These directional, non-covalent interactions—formed between hydrogen bond donors and acceptors on the protein and ligand—contribute substantially to the binding free energy and are critical for stabilizing the complex. A well-organized hydrogen-bond network helps maintain the ligand in an optimal orientation within the binding pocket, thereby supporting efficient biological activity (Fu et al., 2018).

In the BMDB0012305–MRGPRD complex, five stable hydrogen bonds were consistently observed throughout the simulation, highlighting the strong interaction network that contributes to complex stability. To further quantify binding strength, binding free energies were calculated using the MM-PBSA (Molecular Mechanics Poisson–Boltzmann Surface Area) method. In this framework, the total binding free energy ($\Delta G_{\text{binding}}$) is computed using the following relationship (Genheden & Ryde, 2015):

$$\Delta G_{\text{binding}} = G_{\text{complex}} - (G_{\text{receptor}} + G_{\text{ligand}})$$

Where, G_{complex} represents the free energy of the bound system, G_{receptor} the free energy of the unbound receptor, and G_{ligand} the free energy of the unbound ligand.

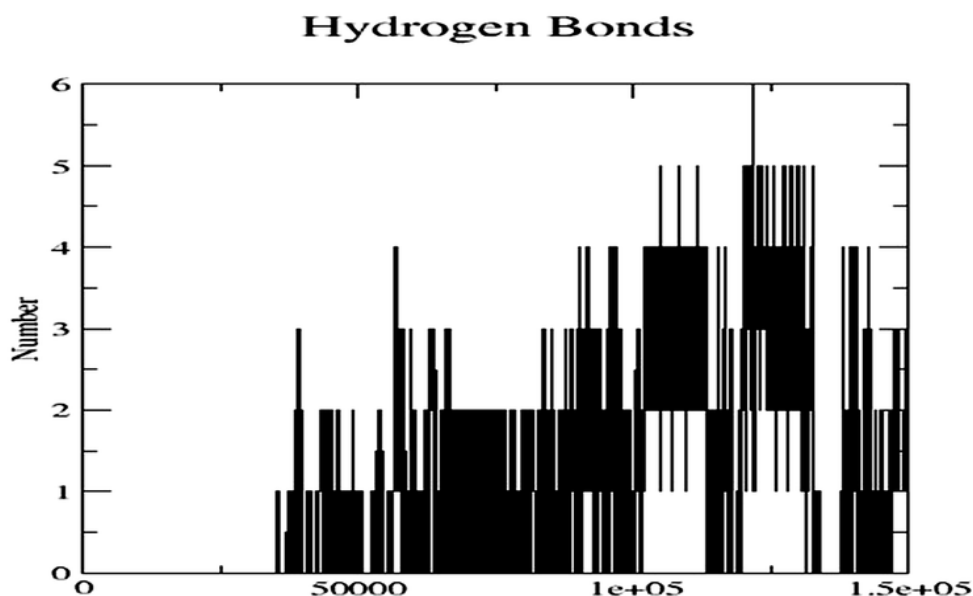


Fig. 6 Intermolecular hydrogen-bond profile of the BMDB0012305–MRGPRD complex.

The hydrogen-bond analysis revealed a pronounced increase in hydrogen-bonding events between simulation frames 215 and 250 (Fig. 6), indicating the formation of a stable and persistent hydrogen-bond network within the BMDB0012305–MRGPRD complex. Hydrogen bonds were identified based on standard geometric criteria involving donor–hydrogen–acceptor angles and interatomic distances, ensuring accurate detection of stabilizing interactions.

The consistency of hydrogen-bond formation throughout the simulation strongly correlates with the overall structural stability of the complex. This observation reinforces the concept that a higher number of persistent hydrogen bonds contributes directly to enhanced protein–ligand stability (Yadav et al., 2023). These findings further support the conclusion that the BMDB0012305–MRGPRD complex maintains a stable conformation during MD simulations and is energetically favorable.

4 Conclusion

MRGPRD, a member of the G protein–coupled receptor (GPCR) family, plays a pivotal role in several physiological processes, including inflammatory signaling, sensory perception, and regulation within the renin–angiotensin system (RAS). In this study, computational screening of cow-milk metabolites against MRGPRD identified BMDB0012305 as the strongest binder, exhibiting the highest docking affinity among all 206 metabolites evaluated. Molecular dynamics simulations conducted over 150 ns further validated this interaction. RMSD, RMSF, and Rg analyses consistently demonstrated that the BMDB0012305–MRGPRD complex remains structurally stable after initial equilibration, indicating a strong and sustained interaction between the ligand and receptor. The presence of stable hydrogen bonds and favorable interaction energies reinforces the robustness of this binding event.

Collectively, these computational findings suggest that BMDB0012305 has the potential to modulate the structural and functional behavior of MRGPRD. Given the receptor’s involvement in RAS-mediated physiological processes, such modulation may influence downstream signaling pathways and could contribute to altered or abnormal physiological responses. While these results provide important theoretical insights,

experimental validation—including biochemical binding assays and functional studies—is essential to confirm the biological relevance of these interactions.

Acknowledgements

NK and SV thank UGC for providing the UGC-CRET fellowship. Neelam Krishna & Shraddha Vishwakarma have contributed equally to this work.

References

- Bader, M., Alenina, N., Andrade-Navarro, M. A., Santos, R. A. 2014. MAS and its related G protein-coupled receptors, *Mgprs*. *Pharmacological Reviews*, 66 (4): 1080–1105. <https://doi.org/10.1124/pr.113.008136>
- Benigni, A., Cassis, P., Remuzzi, G. 2010. Angiotensin II revisited: New roles in inflammation, immunology and aging. *EMBO Molecular Medicine*, 2(7): 247–257. <https://doi.org/10.1002/emmm.201000080>
- Cantero-Navarro, E., Fernández-Fernández, B., Ramos, A. M., Rayego-Mateos, S., Rodrigues-Diez, R. R., Sánchez-Niño, M. D., Sanz, A. B., Ruiz-Ortega, M., Ortiz, A. 2021. Renin-angiotensin system and inflammation update. *Molecular and Cellular Endocrinology*, 529: 111254. <https://doi.org/10.1016/j.mce.2021.111254>
- Di Cera, E. 2020. Mechanisms of ligand binding. *Biophysical Reviews*, 1 (1): 011303.
- Dixit, S., Srivastava, M., Katara, P. 2024. In silico and in vitro assessment of virulent proteins of Fusarium wilt in tomato and identification, designing of new Trichoderma compounds. *Indian Journal of Pharmaceutical Sciences*, 86(4): 1499–1509. <https://doi.org/10.36468/pharmaceutical-sciences.1417>
- Etelvino, G. M., Peluso, A. A., Santos, R. A. 2014. New components of the renin-angiotensin system: Alamandine and the MAS-related G protein-coupled receptor D. *Current Hypertension Reports*, 16(6): 433. <https://doi.org/10.1007/s11906-014-0433-0>
- Fargher, H. A., Sherbow, T. J., Haley, M. M., Johnson, D. W., Pluth, M. D. 2022. C–H···S hydrogen bonding interactions. *Chemical Society Reviews*, 51(4): 1454–1469. <https://doi.org/10.1039/d1cs00838b>
- Fekete, Á. A., Givens, D. I., Lovegrove, J. A. 2015. Casein-derived lactotripeptides reduce systolic and diastolic blood pressure: A meta-analysis of randomised clinical trials. *Nutrients*, 7(1): 659–681. <https://doi.org/10.3390/nu7010659>
- Ferrari, R., Fox, K. 2009. Insight into the mode of action of ACE inhibition in coronary artery disease: The ultimate 'EUROPA' story. *Drugs*, 69(3): 265–277. <https://doi.org/10.2165/00003495-200969030-00003>
- Foroutan, A., Fitzsimmons, C., Mandal, R., Piri-Moghadam, H., Zheng, J., Guo, A., Li, C., Guan, L. L., Wishart, D. S. 2020. The Bovine Metabolome. *Metabolites*, 10(6): 233. <https://doi.org/10.3390/metabo10060233>
- Forrester, S. J., Booz, G. W., Sigmund, C. D., Coffman, T. M., Kawai, T., Rizzo, V., Scalia, R., Eguchi, S. 2018. Angiotensin II signal transduction: An update on mechanisms of physiology and pathophysiology. *Physiological Reviews*, 98(3): 1627–1738
- Fountain, J. H., Kaur, J., Lappin, S. L. 2024. Physiology, renin-angiotensin system. In: StatPearls. StatPearls Publishing.
- Fu, Y., Zhao, J., Chen, Z. 2018. Insights into the molecular mechanisms of protein–ligand interactions by molecular docking and molecular dynamics simulation: A case of oligopeptide-binding protein. *Computational and Mathematical Methods in Medicine*, 2018: 3502514
- Galiè, M. 2019. RAS as supporting actor in breast cancer. *Frontiers in Oncology*, 9: 1199.

- <https://doi.org/10.3389/fonc.2019.01199>
- Genheden, S., Ryde, U. 2015. The MM/PBSA and MM/GBSA methods to estimate ligand-binding affinities. *Expert Opinion on Drug Discovery*, 10(5): 449–461
- Ghahremanian, S., Rashidi, M. M., Raeisi, K., Toghraie, D. 2022. Molecular dynamics simulation approach for discovering potential inhibitors against SARS-CoV-2: A structural review. *Journal of Molecular Liquids*, 354: 118901
- Gomez, R. A., Sequeira-Lopez, M. L. S. 2018. Renin cells in homeostasis, regeneration and immune defence mechanisms. *Nature Reviews Nephrology*, 14(4): 231–245. <https://doi.org/10.1038/nrneph.2017.186>
- Guterres, H., Park, S. J., Cao, Y., Im, W. 2021. CHARMM-GUI ligand designer for template-based virtual ligand design in a binding site. *Journal of Chemical Information and Modeling*, 61(11): 5336–5342. <https://doi.org/10.1021/acs.jcim.1c01156>
- Jiang, H., Galtes, D., Wang, J., Rockman, H. A. 2022. G protein-coupled receptor signaling: Transducers and effectors. *American Journal of Physiology-Cell Physiology*, 323(3): C731–C748. <https://doi.org/10.1152/ajpcell.00210.2022>
- Kanugula, A. K., Kaur, J., Batra, J., Ankireddypalli, A. R., Velagapudi, R. 2023. Renin-angiotensin system: Updated understanding and role in physiological and pathophysiological states. *Cureus*, 15(6): e40725
- Katara, P. 2014. Potential of bioinformatics as a functional genomics tool: An overview. *Network Modeling Analysis in Health Informatics and Bioinformatics*, 3(1): 1–7
- Krishna, N., Tyagi, S., Katara, P. 2024a. Literature mining based profiling of angiotensin-converting enzyme 2. *Network Biology*, 14(2): 77–88
- Krishna, N., Vishwakarma, S., Katara, P. 2024b. Interaction profiling of cow milk metabolites against human renin-angiotensin system (RAS) proteins. *Network Biology*, 14(4): 293–304
- Kumar, S., Gupta, M. K., Gupta, S. K., Katara, P. 2022. Investigation of molecular interaction and conformational stability of disease concomitant to HLA-DR β 3. *Journal of Biomolecular Structure and Dynamics*, 41(17): 8417–8431. <https://doi.org/10.1080/07391102.2022.2134211>
- Li, J., Qin, Y., Chen, Y., Zhao, P., Liu, X., Dong, H., Zheng, W., Feng, S., Mao, X., Li, C. 2020. Mechanisms of the lipopolysaccharide-induced inflammatory response in alveolar epithelial cell/macrophage co-culture. *Experimental and Therapeutic Medicine*, 20(5): 76. <https://doi.org/10.3892/etm.2020.9204>
- Li, S., Chen, F., Li, Y., Wang, L., Li, H., Gu, G., Li, E. 2022. Rhamnose-containing compounds: Biosynthesis and applications. *Molecules*, 27(16): 5315. <https://doi.org/10.3390/molecules27165315>
- Maruyama, Y., Igarashi, R., Ushiku, Y., Mitsutake, A. 2023. Analysis of protein folding simulation with moving root mean square deviation. *Journal of Chemical Information and Modeling*, 63(5): 1529–1541
- Pandey, S., Dhusia, K., Katara, P., Singh, S., Gautam, B. 2020. An in-silico analysis of deleterious SNPs and molecular dynamics simulation of disease-linked mutations in genes responsible for neurodegenerative disorders. *Journal of Biomolecular Structure and Dynamics*, 38(14): 4259–4272. <https://doi.org/10.1080/07391102.2019.1682047>
- Park, K. M., Cifelli, C. J. 2013. Dairy and blood pressure: A fresh look at the evidence. *Nutrition Reviews*, 71(3): 149–157. <https://doi.org/10.1111/nure.12017>
- Rubak, Y. T., Nuraida, L., Iswantini, D., Prangdimurti, E. 2020. Angiotensin-I-converting enzyme inhibitory peptides in milk fermented by indigenous lactic acid bacteria. *Veterinary World*, 13(2): 345–353. <https://doi.org/10.14202/vetworld.2020.345-353>
- Sneha, P., Doss, C. G. 2016. Molecular dynamics: New frontier in personalized medicine. *Advances in Protein Chemistry and Structural Biology*, 102: 181–224. <https://doi.org/10.1016/bs.apcsb.2015.09.004>
- Sriram, K., Loomba, R., Insel, P. A. 2020. Targeting the renin-angiotensin signaling pathway in COVID-19:

- Unanswered questions, opportunities, and challenges. *Proceedings of the National Academy of Sciences*, 117(47): 29274–29282
- Steele, H. R., Han, L. 2021. The signaling pathway and polymorphisms of Mrgprs. *Neuroscience Letters*, 744: 135562
- Sun, Q. 2022. The hydrophobic effects: Our current understanding. *Molecules*, 27(20): 7009. <https://doi.org/10.3390/molecules27207009>
- Suzuki, S., Iida, M., Hiroaki, Y., Tanaka, K., Kawamoto, A., Kato, T., Oshima, A. 2022. Structural insight into the activation mechanism of MrgD with heterotrimeric Gi-protein revealed by cryo-EM. *Communications Biology*, 5(1): 707. <https://doi.org/10.1038/s42003-022-03668-3>
- Timon, C. M., O'Connor, A., Bhargava, N., Gibney, E. R., Feeney, E. L. 2020. Dairy consumption and metabolic health. *Nutrients*, 12(10): 3040. <https://doi.org/10.3390/nu12103040>
- Trott, O., Olson, A. J. 2010. AutoDock Vina: Improving the speed and accuracy of docking with a new scoring function, efficient optimization, and multithreading. *Journal of Computational Chemistry*, 31(2): 455–461. <https://doi.org/10.1002/jcc.21334>
- Turner, P. J. 2005. XMGRACE (Version 5.1.19). Center for Coastal and Land-Margin Research, Oregon Graduate Institute of Science and Technology, USA
- Yadav, A., Kesharwani, A., Chaurasia, D. K., Katara, P. 2023. Mining of molecular insights of CYP2A6 and its variants complex with coumarin (CYP2A6*-coumarin) using molecular dynamics simulation. *Journal of Biomolecular Structure & Dynamics*, 41(9): 4081–4092. <https://doi.org/10.1080/07391102.2022.2062785>
- Zhang, W. J. 2018. *Fundamentals of Network Biology*. World Scientific Europe, London, UK. <https://doi.org/10.1142/q0149>